World Journal of Applied Chemistry
2017; 2(2): 67-76
http://www.sciencepublishinggroup.com/j/wjac
doi: 10.11648/j.wjac.20170202.14

Characterization of the Physicochemical, Spectral, Thermal and Behavioral Properties of Sodium Selenate: An Effect of the Energy of Consciousness Healing Treatment

Mahendra Kumar Trivedi[1], Alice Branton[1], Dahryn Trivedi[1], Gopal Nayak[1], Michael Peter Ellis[1], James Jeffery Peoples[1], James Joseph Meuer[1], Johanne Dodon[1], John Lawrence Griffin[1], John Suzuki[1], Joseph Michael Foty[1], Judy Weber[1], Julia Grace McCammon[1], Karen Brynes Allen[1], Kathryn Regina Sweas[1], Lezley Jo-Anne Wright[1], Lisa A. Knoll[1], Madeline E. Michaels[1], Margaret Kweya Wahl[1], Mark E. Stutheit[1], Michelle Barnard[1], Muriel Mae Ranger[1], Paromvong Sinbandhit[1], V. J. Kris Elig[1], Kalyan Kumar Sethi[2], Parthasarathi Panda[2], Snehasis Jana[2, *]

[1]Trivedi Global, Inc., Henderson, USA

[2]Trivedi Science Research Laboratory Pvt. Ltd., Bhopal, India

Email address:

publication@trivedieffect.com (S. Jana)

[*]Corresponding author

To cite this article:

Mahendra Kumar Trivedi, Alice Branton, Dahryn Trivedi, Gopal Nayak, Michael Peter Ellis, James Jeffery Peoples, James Joseph Meuer, Johanne Dodon, John Lawrence Griffin, John Suzuki, Joseph Michael Foty, Judy Weber, Julia Grace McCammon, Karen Brynes Allen, Kathryn Regina Sweas, Lezley Jo-Anne Wright, Lisa A. Knoll, Madeline E. Michaels, Margaret Kweya Wahl, Mark E. Stutheit, Michelle Barnard, Muriel Mae Ranger, Paromvong Sinbandhit, V. J. Kris Elig, Kalyan Kumar Sethi, Parthasarathi Panda, Snehasis Jana. Characterization of the Physicochemical, Spectral, Thermal and Behavioral Properties of Sodium Selenate: An Effect of the Energy of Consciousness Healing Treatment. *World Journal of Applied Chemistry*. Vol. 2, No. 2, 2017, pp. 67-76. doi: 10.11648/j.wjac.20170202.14

Received: February 27, 2017; **Accepted**: April 13, 2017; **Published**: May 2, 2017

Abstract: Sodium selenate is a source of an essential nutrient selenium used for the prevention and treatment of cancer, heart diseases, viral diseases, diabetes, infectious diseases, etc. The aim of the study was to investigate the impact of Energy of Consciousness Healing Treatment (The Trivedi Effect®) on the physico-chemical, thermal, and behavioral properties of sodium selenate using PXRD, PSD, FT-IR, UV-vis, TGA, and DSC analysis. Sodium selenate was divided into two parts – one part was control/untreated sample, while another part was treated with Energy of Consciousness Healing Treatment remotely by twenty renowned Biofield Energy Healers and defined as the treated sample. The PXRD diffractograms showed sharp and intense peaks in both the samples, indicated both the samples were crystalline in nature. The crystallite size of the treated sample was significantly altered in the range of -16.66% to 50.07% compared with the control sample. Consequently, the average crystallite size of the treated sample was significantly increased by 9.57% compared to the control sample. The particle size of the treated sample at d_{10}, d_{50}, and d_{90} values were significantly increased by 9.47%, 19.06%, and 27.81%, respectively compared with the control sample. Thus, the surface area of the treated sample was significantly decreased by 9.16% compared to the control sample. The control and treated FT-IR spectra indicated the presence of sharp and strong absorption bands at 888 cm^{-1} due to the Se=O stretching. The wavelength of the maximum absorbance of the control and Biofield Energy Treated sodium selenate were at 206.3 nm and 205.9 nm, respectively in UV-vis spectroscopy. TGA analysis indicated that the total weight loss of the treated sample was reduced by 0.71% compared to the control sample. The DSC analysis showed that the vaporization temperature of the treated sample (94.97°C) was slightly decreased compared to the control sample (95.30°C). But, the latent heat of vaporization was significantly increased in the treated sample by 45.31% compared to the control sample. Thus, The Trivedi Effect® might lead to generate a new polymorphic form of sodium selenate, which would have better powder flowability and long-term storage stability compared with the control sample. The Biofield Energy Treated sodium selenate would be very useful to design better nutraceutical and pharmaceutical formulations which might offer a better therapeutic response against cancer, inflammatory diseases, infectious diseases, immunological disorders, stress, aging, Alzheimer's disease, heart diseases, viral diseases, diabetes, infectious diseases, etc.

Keywords: The Trivedi Effect®, Biofield Energy Healers, Consciousness Energy Healing Treatment, Sodium Selenate, PXRD, Particle Size, TGA, DSC

1. Introduction

In the human body, selenium is an essential trace nutrient that plays an important role in the biological functions, *i.e.* catalytic effect on the metabolite reaction of intermediate and inhibit the toxic effect of heavy metals. Selenium is actively present in the active site of enzymes and in more than 30 proteins. It acts as a potent antioxidant for the cellular defense mechanism against free radicals [1, 2]. Selenium deficiency leads to several disorders, i.e. cancer, infectious diseases, heart diseases, diabetes, viral diseases, degenerative ailments, etc. The therapeutic window of selenium is very small between essentiality and toxicity. A little bit high concentration of selenium may affect the human health such as irritation of the skin, eye, loosing hair and nails; which may cause cancer, giddiness, depression, nervousness, etc. [1-3]. The different chemical forms of selenium have an impact on its solubility and availability in the organisms. Among selenium compounds, selenate is the most oxidized form with less toxicity and higher water solubility [1-5]. It can be useful for the prevention and treatment of Alzheimer's disease, inflammatory diseases, etc. [6-8]. Similarly, sodium selenate also used in the glass industry [9], preparation of some insecticides (aphids, against mites, and mealybugs) and fungicides [10, 11]. Sodium selenate in combination with vitamin E can prevent many nutritional deficiency diseases. Inorganic forms of selenium after absorption in the body undergo reductive metabolism giving H_2Se, which is responsible for the production of selenoproteins [12]. Therefore, sodium selenate was added as one of the components in a novel test formulation prepared as a source of selenium ion, along with zinc chloride, magnesium gluconate, and *Withania somnifera* root extract. This novel herbomineral formulation can also be used for the prevention and treatment of various human disorders.

Every human being can discharge electromagnetic waves in the form of bio-photons that surrounds the body. This electromagnetic energy is generated due to the continuous movement of the electrically charged particles (i.e. cells, ions, etc.) inside the body, collectively known as "Biofield Energy". The Biofield Energy Healing practitioners have the ability to harness the energy from the "universal energy field" or the environment and that can be transmit into any living or nonliving object(s). The process by which the objects receive the Biofield Energy and respond in a useful way is called as Biofield Energy Healing [13-15]. Biofield (Putative Energy Fields) based Energy Therapies have recognized and accepted as a Complementary and Alternative Medicine (CAM) by the National Center of Complementary and Integrative Health (NCCIH) in addition to other therapies, medicines and practices such as Ayurvedic medicine, traditional Chinese herbs and medicines, essential oils, aromatherapy, yoga, meditation, Tai Chi, Qi Gong, chiropractic/osteopathic manipulation, massage, homeopathy, progressive relaxation, acupressure, acupuncture, hypnotherapy, Reiki, healing touch, relaxation techniques, movement therapy, pilates, rolfing structural integration, cranial sacral therapy and applied prayer (common in all religions, like Hinduism, Christianity, Buddhism, Judaism, etc.) [16]. The Biofield Energy Healing Treatment (also known as The Trivedi Effect®) has the astounding capability for alteration of the characteristic properties of the several living organisms and non-living materials. The impact of The Trivedi Effect® - Biofield Energy Healing Treatment scientifically studied and has been proven in various fields including materials science [17, 18], organic compounds [19-21], microbiology [22-24], agricultural [25, 26], biotechnology [27-29], genetics [30, 31], nutraceuticals [32, 33], pharmaceuticals [34, 35]. As per the literature bioavailability of inorganic selenium is lower than the organic forms of selenium [12]. The physicochemical properties such as crystalline structure, crystallite size, particle size, surface area, etc. of a drug molecule play an important role in solubility and bioavailability [36]. The particle size, specific surface area, crystalline nature, chemical and thermal behavior of an atom/ion might be altered by The Trivedi Effect® - Biofield Energy Healing Treatment through the possible mediation of neutrinos [37]. Hence, the aim of the present study was to evaluate the effects of the Biofield Energy Healing Treatment on the physicochemical, spectral, and thermal properties of sodium selenate using various analytical techniques include powder X-ray diffraction (PXRD), particle size distribution analysis (PSD), Fourier transform infrared (FT-IR) spectrometry, ultraviolet-visible (UV-vis) spectroscopy, thermogravimetric analysis (TGA), and differential scanning calorimetry (DSC) analysis.

2. Materials and Methods

2.1. Chemicals and Reagents

Sodium selenate was procured from Alfa Aesar, USA. All other chemicals used in the experiment were of analytical grade available in India.

2.2. Consciousness Energy Healing Treatment Strategies

Sodium selenate was one of the components of the new proprietary herbomineral formulation, and it was used *per se* as a test compound for the present study. The test compound was divided into two parts. One part of the test compound did not receive any Biofield Energy Treatment and was defined as the untreated or control sodium selenate sample. The second part of the test compound was treated with Energy of Consciousness Healing Treatment (The Trivedi Effect®) by a

group of twenty renowned Biofield Energy Healers remotely and indicated as the Biofield Energy Treated sample. Thirteen Biofield Energy Healers were remotely located in the U. S. A., five were located in Canada, and two were located in Australia, while the test compound was located in the research laboratory of GVK Biosciences Pvt. Ltd., Hyderabad, India. This Biofield Energy Treatment was provided for 5 minutes through Healer's Unique Energy Transmission process remotely to the test compound under the laboratory conditions. None of the Biofield Energy Healers in this study visited the laboratory in person, nor had any contact with the compounds. Similarly, the control compound was subjected to "sham" healers for 5 minutes, under the same laboratory conditions. The sham healer did not have any knowledge about Energy of Consciousness Healing Treatment (The Trivedi Effect®). After that, the treated and untreated samples were kept in similar sealed conditions for the characterization using PXRD, PSD, FT-IR, UV-visible spectroscopy, TGA, and DSC analysis.

2.3. Characterization

2.3.1. Powder X-ray Diffraction (PXRD) Analysis

The PXRD analysis was performed on PANalytical X'Pert Pro powder X-ray diffractometer system. The XRD conditions and the sample preparation was followed as per the recent literature [38-40]. The crystallite size (G) was calculated from the Scherrer equation [41, 42]. The crystallite size (G) was calculated by using the following equation (1):

$$G = k\lambda/(bCos\theta) \quad (1)$$

Where, k is the equipment constant (0.5), λ is the X-ray wavelength (0.154 nm); b in radians is the full-width at half of the peaks and θ the corresponding Bragg angle.

Percent change in crystallite size (G) was calculated using following equation (2):

$$\%\ \text{change in crystallite size} = \frac{[G_{Treated} - G_{Control}]}{G_{Control}} \times 100 \quad (2)$$

Where, $G_{Control}$ and $G_{Treated}$ are the crystallite size of the control and Biofield Energy Treated samples, respectively.

2.3.2. Particle Size Distribution (PSD) Analysis

The average particle size and particle size distribution were analyzed using Malvern Mastersizer 2000, UK. The PSD conditions and the sample preparation was followed as per the recent literature [38-40].

The percent change in particle size (d) for at below 10% level (d_{10}), 50% level (d_{50}), and 90% level (d_{90}) was calculated using following equation (3):

$$\%\ \text{change in particle size} = \frac{[d_{Treated} - d_{Control}]}{d_{Control}} \times 100 \quad (3)$$

Where, $d_{Control}$ and $d_{Treated}$ are the particle size (μm) for at below 10% level (d_{10}), 50% level (d_{50}), and 90% level (d_{90}) of the control and Biofield Energy Treated samples, respectively.

Percent change in surface area (S) was calculated using following equation (4):

$$\%\ \text{change in surface area} = \frac{[S_{Treated} - S_{Control}]}{S_{Control}} \times 100 \quad (4)$$

Where, $S_{Control}$ and $S_{Treated}$ are the surface area of the control and Biofield Energy Treated samples, respectively.

2.3.3. Fourier Transform Infrared (FT-IR) Spectroscopy

FT-IR spectroscopy of sodium selenate was performed on Spectrum two (Perkin Elmer, USA) Fourier transform infrared spectrometer by using pressed KBr disk technique [38-40].

2.3.4. Ultraviolet-visible Spectroscopy (UV-Vis) Analysis

The UV-Vis spectral analysis was carried out using Shimadzu UV-2450 with UV Probe, Japan. The absorbance spectra and wavelength of maximum absorbance (λ_{max}) were recorded [38-40].

2.3.5. Thermal Gravimetric Analysis (TGA)

TGA analysis was performed using instrument TGA Q50 (TA Instruments, USA) taking 11.283 mg of control and 15.79 mg of Biofield Energy Treated samples, and the remaining TGA conditions were followed as per the recent literature [38-40]. The % change in weight loss (W) was calculated using following equation (5):

$$\%\ \text{change in weight loss} = \frac{[W_{Treated} - W_{Control}]}{W_{Control}} \times 100 \quad (5)$$

Where, $W_{Control}$ and $W_{Treated}$ are the weight loss of the control and Biofield Energy Treated samples, respectively.

2.3.6. Differential Scanning Calorimetry (DSC)

The analysis was performed using the DSC Q20 (TA Instruments, USA) using ~5 mg of samples. The remaining DSC conditions were followed as per the recent literature [38-40]. The % change in melting point (T) was calculated using following equation (6):

$$\%\ \text{change in melting point} = \frac{[T_{Treated} - T_{Control}]}{T_{Control}} \times 100 \quad (6)$$

Where, $T_{Control}$ and $T_{Treated}$ are the melting point of the control and treated samples, respectively.

Percent change in the latent heat of fusion (ΔH) was calculated using following equation (7):

$$\%\ \text{change in latent heat of fusion} = \frac{[\Delta H_{Treated} - \Delta H_{Control}]}{\Delta H_{Control}} \times 100 \quad (7)$$

Where, $\Delta H_{Control}$ and $\Delta H_{Treated}$ are the latent heat of fusion of the control and treated samples, respectively.

3. Results and Discussion

3.1. Powder X-Ray Diffraction (PXRD) Analysis

The PXRD diffractograms of the control and Biofield Energy Treated sodium selenate showed very sharp and intense peaks (Figure 1) indicating that both these samples were crystalline in nature. The PXRD diffractograms showed

the significant alterations in the crystallite size of the treated sodium selenate compared with the control sample. From Table 1 (entry 1), the most intense peaks for the control and treated samples were found at 2θ equal to 18.4°. The crystallite size of the Biofield Energy Treated sodium selenate at 2θ equal to nearly 18.4°, 22.5°, 27.3°, 32.6°, and 37.2° (Table 1, entry 1-3, 6, and 7) was significantly increased from 12.56% to 50.07% compared with the control sample. Consequently, at position 2θ equal to nearly 57.2° (Table 1, entry 11) the crystallite size values of the Biofield Energy Treated samples were markedly decreased by 16.66% in comparison to the control sample. But, the crystallite size of the control and Biofield Energy Treated sodium selenate at 2θ equal to nearly 28.4°, 31.0°, 47.4°, 48.8°, and 52.9° (Table 1, entry 3, 4, and 8-10) were the same value. Overall, the average crystallite size of the Biofield Energy Treated sodium selenate was significantly increased by 9.57% compared with the control sample.

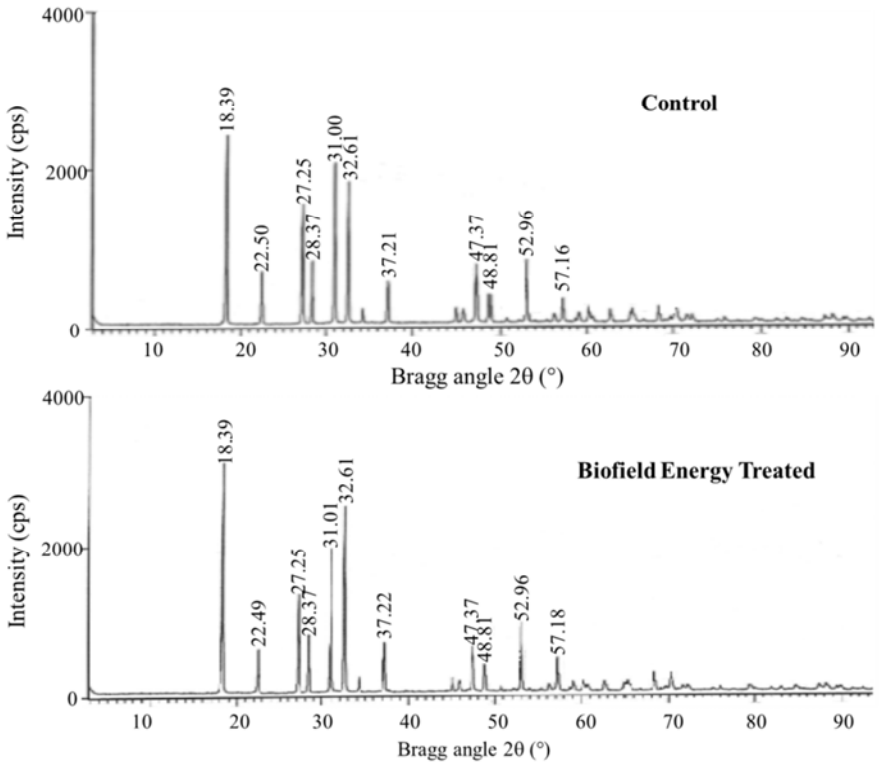

Figure 1. *PXRD diffractograms of the control and Biofield Energy Treated sodium selenate.*

Table 1. *PXRD data for the control and Biofield Energy Treated sodium selenate.*

Entry No.	Bragg angle (°2θ)		Relative Intensity (%)		FWHM (°2θ)		Crystallite size (G, nm)		
	Control	Treated	Control	Treated	Control	Treated	Control	Treated	% change*
1	18.39	18.39	100.00	100.00	0.1004	0.0836	44.41	53.34	20.10
2	22.50	22.49	28.07	19.63	0.1338	0.1171	33.54	38.33	14.26
3	27.25	27.25	63.43	42.93	0.1338	0.1004	33.85	45.12	33.27
4	28.37	28.37	33.60	25.65	0.1004	0.1004	45.23	45.23	0.00
5	31.00	31.01	84.63	62.20	0.1004	0.1004	45.50	45.51	0.00
6	32.61	32.61	74.40	80.64	0.1004	0.0669	45.69	68.57	50.07
7	37.21	37.22	22.41	21.98	0.1506	0.1338	30.85	34.72	12.56
8	47.37	47.37	30.75	19.19	0.1020	0.1020	47.15	47.15	0.00
9	48.81	48.81	15.09	11.33	0.1224	0.1224	39.51	39.51	0.00
10	52.96	52.96	32.54	29.41	0.1224	0.1224	40.20	40.20	0.00
11	57.16	57.18	12.31	14.94	0.1020	0.1224	49.18	40.98	-16.66
12	Average crystallite size						41.37	45.33	9.57

FWHM: Full width half maximum, *denotes the percentage change in the crystallite size of Biofield Energy Treated sample with respect to the control sample.

The PXRD parameters such as relative intensities of the peaks in the Biofield Energy Treated sample were significantly altered compared to the control sample. The relative intensity of each XRD diffraction face on crystalline compound changes with the crystal morphology [43] and the alterations in the XRD pattern provide the proof of polymorphic transitions [44-46]. Hence, alteration in the crystallite size and relative intensities of XRD peaks revealed that the crystal morphology of the treated sample was modified compared with the control sample. Thus, it can be assumed that the alteration in the crystal morphology of the sodium selenate was due to the Biofield Energy Healing

Treatment and this probably introduced a new polymorphic form of sodium selenate. The crystal size and even polymorphic form of a drug molecule have the important effect on drug solubility, dissolution, and bioavailability [47]. Therefore, it is inferred that The Trivedi Effect® - Biofield Energy Healing Treatment would be helpful to improve the bioavailability of sodium selenate.

3.2. Particle Size Distribution (PSD) Analysis

Particle size values and surface area of the control and Biofield Energy Treated sodium selenate were are presented in Table 2. The particle size values of the control sample were 5.07 µm (d_{10}), 23.19 µm (d_{50}), and 64.14 µm (d_{90}). Similarly, the particle size values of the Biofield Energy Treated sodium selenate were 5.55 µm (d_{10}), 27.61 µm (d_{50}), and 81.98 µm (d_{90}). Thus, the particle size values at d_{10}, d_{50}, and d_{90} of the Biofield Energy Treated sample were significantly increased by 9.47%, 19.06%, and 27.81%, respectively compared with the control sample. The surface area of the Biofield Energy Treated sodium selenate (0.45 m^2/g) was significantly decreased by 9.16% compared with the control sample (0.49 m^2/g).

Table 2. *Particle size data (d_{10}, d_{50}, and d_{90}) and surface area of the control and Biofield Energy Treated sodium selenate.*

Parameter	d_{10} (µm)	d_{50} (µm)	d_{90} (µm)	Surface area (m^2/g)
Control	5.07	23.19	64.14	0.49
Biofield Treated	5.55	27.61	81.98	0.45
Percent change* (%)	9.47	19.06	27.81	-9.16

*denotes the percentage change in the particle size data (d_{10}, d_{50}, and d_{90}) and surface area of Biofield Energy Treated sample with respect to the control sample.

The particle shape, size, and surface area of a compound play an important role in the solubility, dissolution and bioavailability of the pharmaceuticals [36, 48]. The various reasons to increase the particle size are enhanced flowability, improved product shape and appearance [49, 50]. It is assumed that Biofield Energy Healing Treatment might improve the flowability, size and surface area of sodium selenate.

3.3. Fourier Transform Infrared (FT-IR) Spectroscopy

The FT-IR spectra of the control and Biofield Energy Treated samples of sodium selenate are presented in Figure 2. The characteristic absorption bands in the 3800-3200 cm^{-1} and 1700-1600 cm^{-1} regions due to the O-H stretching and bending, respectively for the water molecules assimilated into the lattice structure of the crystalline inorganic compounds [51]. The control IR spectrum displayed the O-H stretching and bending absorption bands at 3438, 1723, and 1639 cm^{-1}, respectively. In addition, peaks for the O-H stretching and bending of the water molecules in the Biofield Energy Treated sample were found at 3450, 1724, and 1631 cm^{-1}. The fingerprint region of the Biofield Energy Treated and control samples was remained unchanged. From the literature, it has been found that M=O (metal-oxide) stretching absorption band for inorganic materials was found in the 1010-850 cm^{-1} region [51]. A sharp and strong absorption bands at 888 cm^{-1} due to the Se=O stretching were found in case of both the sample. The FT-IR results indicated that the structure of the Biofield Energy Treated sodium selenate was remained same with respect to the control sample.

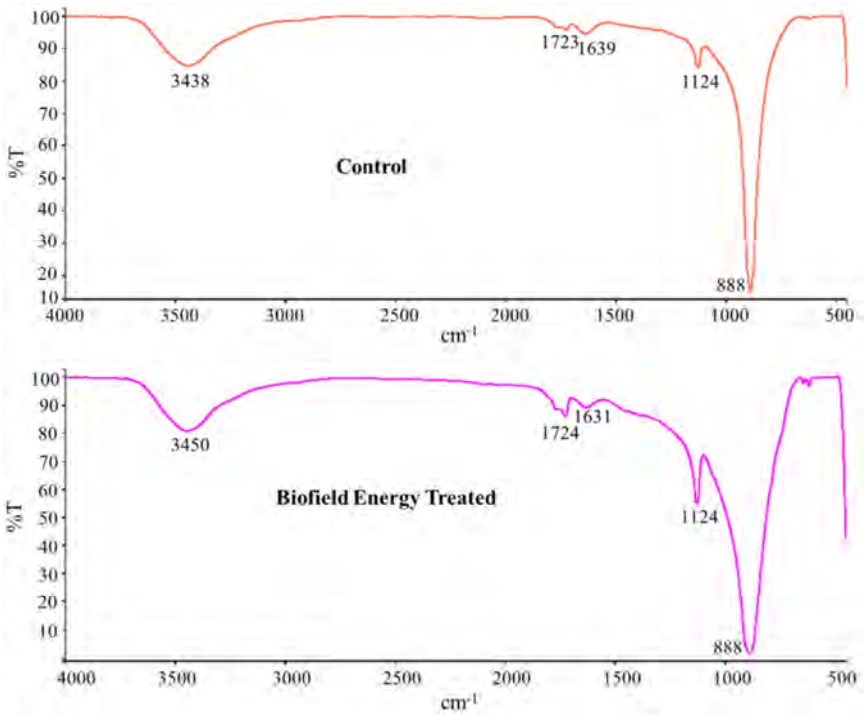

Figure 2. *FT-IR spectra of the control and Biofield Energy Treated sodium selenate.*

3.4. Ultraviolet-Visible Spectroscopy (UV-Vis) Analysis

The wavelength of maximum absorbance (λ_{max}) of the control and Biofield Energy Treated sodium selenate were at 206.3 nm and 205.9 nm, respectively and there was a minor move of absorbance maxima from 2.4825 in the control sample to 2.3240 in the Biofield Energy Treated sample. There was no change in the λ_{max} of the Biofield Energy Treated sample as compared to the control sample. It is anticipated that the structural configuration or activation energy of sodium selenate remained unchanged after The Trivedi Effect® - Biofield Energy Healing Treatment.

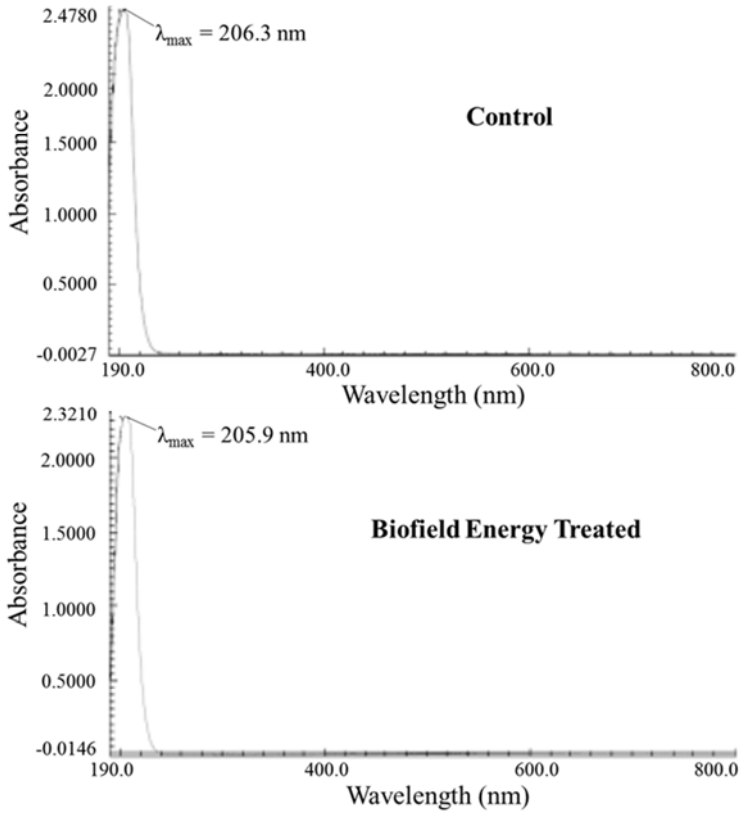

Figure 3. *UV-vis spectra of the control and Biofield Energy Treated sodium selenate.*

3.5. Thermal Gravimetric Analysis (TGA)

The TGA and DSC analysis were used to examine the thermal stability of the control and Biofield Energy Treated sodium selenate (Figure 4). The thermal stability of a solid compound plays an important role in the stability, quality, efficacy, and safety in a drug formulation during the manufacturing process, handling, shipment, and storage [52]. The TGA analysis showed one steps of thermal degradation of the control and Biofield Energy Treated sodium selenate.

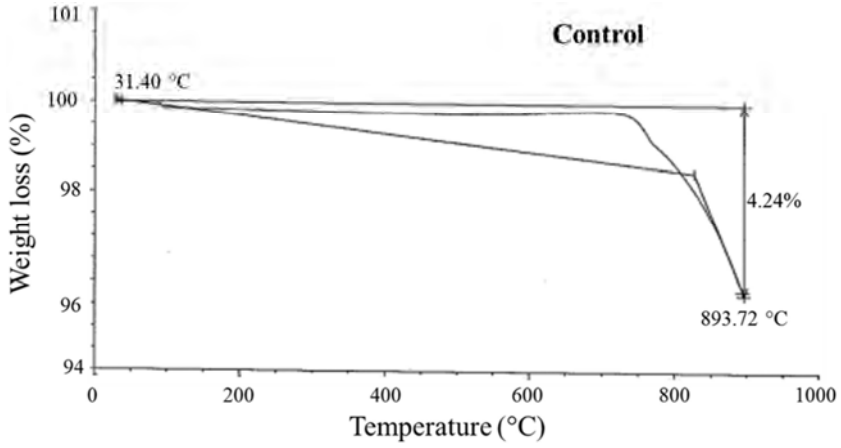

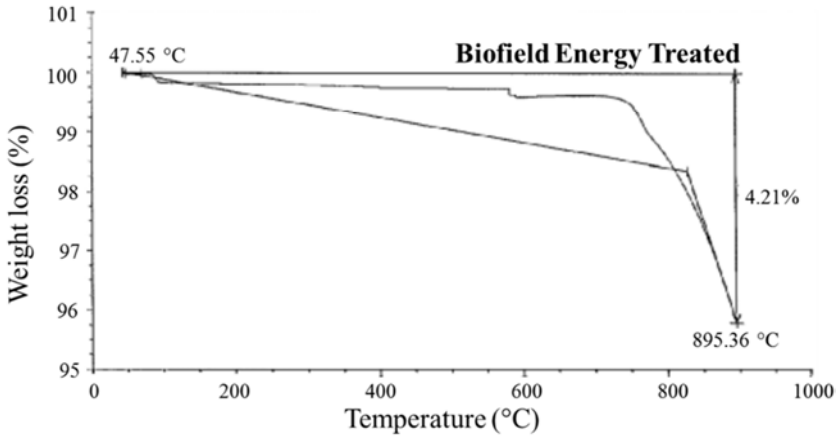

Figure 4. *TGA thermograms of the control and Biofield Energy Treated sodium selenate.*

The TGA thermogram of the control sample exhibited 4.24% weight loss from 31.40°C to 893.72°C. Consequently, the TGA thermogram of the Biofield Energy Treated sample showed 4.21% weight loss from 47.55°C to 895.36°C. The weight loss of the Biofield Energy Treated sample was reduced by 0.71% compared with the control sample. Thus, it is assumed that The Trivedi Effect® - Consciousness Energy Healing Treatment might improve the thermal stability of sodium selenate.

3.6. Differential Scanning Calorimetry (DSC) Analysis

The DSC thermogram of the control sample showed the presence of a sharp endothermic inflection at 95.30°C which was due to evaporation of the bound water and the latent heat of vaporization ($\Delta H_{vaporization}$) was 2.56 J/g (Figure 5 and Table 3). Consequently, the Biofield Energy Treated sodium selenate showed this endothermic peak at 94.97°C along with $\Delta H_{vaporization}$ of 3.72 J/g. This suggested that the temperature of the evaporation of the bound water in the Biofield Energy Treated sample was slightly (0.35%) decreased, whereas the $\Delta H_{vaporization}$ was significantly increased by 45.31% compared to the control sample. Therefore, it is assumed that The Trivedi Effect® - Consciousness Energy Healing Treatment might improve the thermal stability of sodium selenate.

Table 3. *Comparison of DSC data between the control and Biofield Energy Treated sodium selenate.*

Sample	Onset vaporization temperature (T_{onset})°C	Peak vaporization temperature (T_{peak})°C	Endset vaporization temperature (T_{endset})°C	Latent heat of vaporization ($\Delta H_{vaporization}$) J/g
Control	89.93	95.30	100.08	2.56
Biofield Energy Treated	88.66	94.97	101.25	3.72
% Change*	-1.41	-0.35	1.17	45.31

T_{onset}: Onset vaporization temperature, T_{peak}: Peak vaporization temperature, T_{endset}: Endset vaporization temperature, $\Delta H_{vaporization}$: Latent heat of vaporization, *denotes the percentage change of Biofield Energy Treated sample with respect to the control sample.

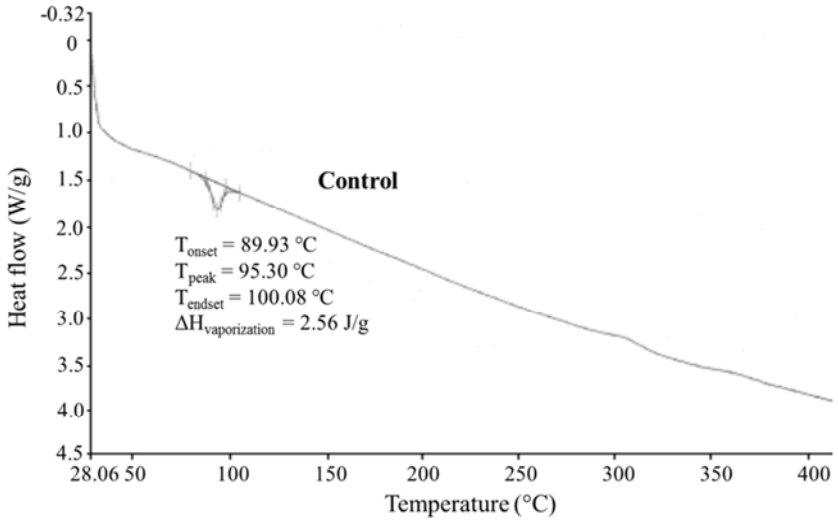

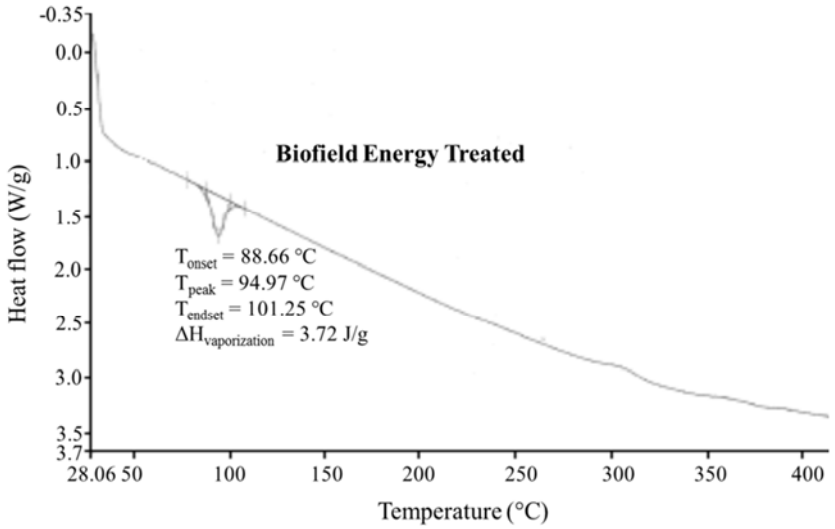

Figure 5. *DSC thermograms of the control and Biofield Energy Treated sodium selenate.*

4. Conclusions

The experimental results revealed that Energy of Consciousness Healing Treatment (The Trivedi Effect®) displayed the significant impact on the physico-chemical, thermal, and behavioral properties of sodium selenate. The PXRD analysis showed the remarkable alteration of the crystallite size of the treated sample from -16.66% to 50.07% compared with the control sample. Overall, the average crystallite size of the Biofield Energy Treated sodium selenate was significantly increased by 9.57% compared with the control sample. This result indicated that the crystal morphology of the treated sodium selenate was changed from the control sample and The Trivedi Effect® - Biofield Energy Healing Treatment might lead to a new polymorphic form of sodium selenate. The particle size of the Biofield Energy Treated sample at d_{10}, d_{50}, and d_{90} values were significantly increased by 9.47%, 19.06%, and 27.81%, respectively compared with the control sample. Therefore, the surface area of the treated sample was significantly decreased by 9.16% compared with the control sample. TGA analysis revealed that the total weight loss of the Biofield Energy Treated sample was reduced by 0.71% compared with the control sample. The DSC analysis revealed that the vaporization temperature of the treated sample (94.97°C) was decreased slightly compared to the control sample (95.30°C). The latent heat of vaporization was increased significantly in the Biofield Energy Treated sample by 45.31% compared to the control sample. The TGA and DSC analysis revealed that the Biofield Energy Treated sample might have improved thermal stability compared with the control sample. Briefly, the Biofield Energy Treated sodium selenate might be a new polymorphic form of sodium selenate having increased crystallite/particle size, and decreased surface area. Thus, The Trivedi Effect® - Biofield Energy Treated sodium selenate could be better powder flowability and long-term storage stability compared with the control sample. Hence, The Trivedi Effect® treated sodium selenate would be useful to design better nutraceutical and pharmaceutical formulations that might offer better therapeutic response against various diseases such as diabetes mellitus, allergies, septic shock, insomnia, anxiety, depression, Attention Deficit Disorder, Attention Deficit Hyperactive Disorder, mental restlessness, brain frog, low libido, impotency, lack of motivation, mood swings, confusion, migraines, headaches, forgetfulness, overwhelm, worthlessness, loneliness, indecisiveness, frustration, irritability, chronic fatigue, Lupus, Systemic Lupus Erythematosus, Hashimoto Thyroiditis, Asthma, Chronic peptic ulcers, Tuberculosis, Hepatitis, Chronic active hepatitis, Celiac Disease, Addison Disease, Crohn's disease, Graves' Disease, Pernicious and Aplastic Anemia, Sjogren Syndrome, Irritable Bowel Syndrome, Arthritis, osteoporosis, Chronic periodontitis, Multiple Sclerosis, Ulcerative colitis, Chronic sinusitis, Myasthenia Gravis, Atherosclerosis, Vasculitis, Dermatitis, Diverticulitis, Alopecia Areata, Psoriasis, Scleroderma, Fibromyalgia, Chronic Fatigue Syndrome and Vitiligo, cardiovascular disease, cancer, Alzheimer's disease, dementia, cataracts, hypertension, glaucoma, hearing loss, Parkinson's Disease, Huntington's Disease, Prion Disease, Motor Neuron Disease, Spinocerebellar Ataxia, Spinal muscular atrophy, Friedreich's Ataxia, Amyotrophic lateral sclerosis, Lewy Body Disease, chronic infections and much more.

Abbreviations

DSC: Differential scanning calorimetry, FT-IR: Fourier transform infrared spectroscopy, FWHM: Full width half maximum, G: Crystallite size, HOMO: Highest energy occupied molecular orbital, LUMO: Lowest energy unoccupied molecular orbital, TGA: Thermal gravimetric analysis, T_{onset}: Onset melting temperature, T_{peak}: Peak melting temperature, T_{endset}: Endset melting temperature, $\Delta H_{vaporization}$: Latent heat of vaporization, UV-vis: Ultraviolet-visible spectroscopy, PSD: Particle size distribution, PXRD: Powder X-ray diffraction.

Acknowledgements

The authors are grateful to GVK Biosciences Pvt. Ltd., Trivedi Science, Trivedi Global, Inc. and Trivedi Master Wellness for their assistance and support during this work.

References

[1] Basnayake RST (2001) Inorganic selenium and tellurium speciation in aqueous medium of biological samples, Master of Science (Chemistry), December 2001, Sam Houston State University, Huntsville, Texas, 60 pp.

[2] Soruraddin MH, Heydari R, Puladvand M, Zahedi MM (2011) A new spectrophotometric method for determination of selenium in cosmetic and pharmaceutical preparations after preconcentration with cloud point extraction. Int J Anal Chem 2011: 729651.

[3] UmyFsová D, Vítová M, Doušková I, Bišová K, Hlavová M, Čížková M, Machát J, Doucha J, Zachleder V (2009) Bioaccumulation and toxicity of selenium compounds in the green alga *Scenedesmus quadricauda*. BMC Plant Biol 9: 58.

[4] Gonzalez CM, Hernandez J, Peralta-Videa JR, Botez CE, Parsons JG, Gardea-Torresdey JL (2012) Sorption kinetic study of selenite and selenate onto a high and low pressure aged iron oxide nanomaterial. J Hazard Mater 211-212: 138-145.

[5] Sabaty M, Avazeri C, Pignol D, Vermeglio A (2001) Characterization of the reduction of selenate and tellurite by nitrate reductases. Appl Environ Microbiol 67: 5122-5126.

[6] Van Eersel J, Ke YD, Liu X, Delerue F, Kril JJ, Götz J, Ittner LM (2010) Sodium selenate mitigates tau pathology, neurodegeneration, and functional deficits in Alzheimer's disease models. Proc Natl Acad Sci USA 107: 13888-13893.

[7] Salama RM, Schaalan MF, Elkoussi AA, Khalifa AE (2013) Potential utility of sodium selenate as an adjunct to metformin in treating type II diabetes mellitus in rats: A perspective on protein tyrosine phosphatase. Biomed Res Int 2013: 231378.

[8] Ryan-Harshman M, Aldoori W (2005) The relevance of selenium to immunity, cancer, and infectious/inflammatory diseases. Can J Diet Pract Res 66: 98-102.

[9] https://en.wikipedia.org/wiki/Sodium_selenate.

[10] Krieger RI (2001) Handbook of Pesticide Toxicology, 2nd Edn, Volume 1; Academic Press: San Diego, CA.

[11] Hanson B, Lindblom SD, Loeffler ML, Pilon-Smits E (2004) Selenium protects plants from phloem-feeding aphids due to both deterrence and toxicity. New Phytologist 162: 655-662.

[12] Haug A, Graham RD, Christophersen OA, Lyons GH (2007) How to use the world's scarce selenium resources efficiently to increase the selenium concentration in food. Microb Ecol Health Dis 19: 209-228.

[13] Rubik B (2002) The biofield hypothesis: Its biophysical basis and role in medicine. J Altern Complement Med 8: 703-717.

[14] Nemeth L (2008) Energy and biofield therapies in practice. Beginnings 28: 4-5.

[15] Rivera-Ruiz M, Cajavilca C, Varon J (2008) Einthoven's string galvanometer: The first electrocardiograph. Tex Heart Inst J 35: 174-178.

[16] Koithan M (2009) Introducing complementary and alternative therapies. J Nurse Pract 5: 18-20.

[17] Trivedi MK, Branton A, Trivedi D, Nayak G, Sethi KK, Jana S (2016) Isotopic abundance ratio analysis of biofield energy treated indole using gas chromatography-mass spectrometry. Science Journal of Chemistry 4: 41-48.

[18] Trivedi MK, Branton A, Trivedi D, Nayak G, Panda P, Jana S (2016) Evaluation of the isotopic abundance ratio in biofield energy treated resorcinol using gas chromatography-mass spectrometry technique. Pharm Anal Acta 7: 481.

[19] Trivedi MK, Branton A, Trivedi D, Nayak G, Bairwa K, Jana S (2015) Fourier transform infrared and ultraviolet-visible spectroscopic characterization of ammonium acetate and ammonium chloride: An impact of biofield treatment. Mod Chem Appl 3: 163.

[20] Trivedi MK, Branton A, Trivedi D, Nayak G, Bairwa K, Jana S (2015) Impact of biofield treatment on spectroscopic and physicochemical properties of p-nitroaniline. Insights in Analytical Electrochemistry 1: 1-8.

[21] Trivedi MK, Branton A, Trivedi D, Nayak G, Bairwa K, Jana S (2015) Spectroscopic characterization of disodium hydrogen orthophosphate and sodium nitrate after biofield treatment. J Chromatogr Sep Tech 6: 282.

[22] Trivedi MK, Patil S, Shettigar H, Mondal SC, Jana S (2015) In vitro evaluation of biofield treatment on Enterobacter cloacae: Impact on antimicrobial susceptibility and biotype. J Bacteriol Parasitol 6: 241.

[23] Trivedi MK, Branton A, Trivedi D, Shettigar H, Nayak G, Gangwar M, Jana S (2015) Assessment of antibiogram of multidrug-resistant isolates of Enterobacter aerogenes after biofield energy treatment. J Pharma Care Health Sys 2: 145.

[24] Trivedi MK, Patil S, Shettigar H, Mondal SC, Jana S (2015) Evaluation of biofield modality on viral load of Hepatitis B and C viruses. J Antivir Antiretrovir 7: 083-088.

[25] Trivedi MK, Branton A, Trivedi D, Nayak G, Gangwar M, Jana S (2015) Effect of biofield energy treatment on chlorophyll content, pathological study, and molecular analysis of cashew plant (*Anacardium occidentale L.*). Journal of Plant Sciences 3: 372-382.

[26] Trivedi MK, Branton A, Trivedi D, Nayak G, Mondal SC, Jana S (2015) Morphological characterization, quality, yield and DNA fingerprinting of biofield treated alphonso mango (*Mangifera indica* L.). Journal of Food and Nutrition Sciences 3: 245-250.

[27] Trivedi MK, Branton A, Trivedi D, Nayak G, Bairwa K, Jana S (2015) Physical, thermal, and spectroscopic characterization of biofield energy treated murashige and skoog plant cell culture media. Cell Biology 3: 50-57.

[28] Trivedi MK, Branton A, Trivedi D, Nayak G, Mishra RK, Jana S (2015) Characterization of physical, thermal and spectral properties of biofield treated date palm callus initiation medium. International Journal of Nutrition and Food Sciences 4: 660-668.

[29] Trivedi MK, Branton A, Trivedi D, Nayak G, Mishra RK, Jana S (2015) Comparative physicochemical evaluation of biofield treated phosphate buffer saline and hanks balanced salt medium. American Journal of BioScience 3: 267-277.

[30] Trivedi MK, Patil S, Shettigar H, Bairwa K, Jana S (2015) Evaluation of phenotyping and genotyping characterization of *Serratia marcescens* after biofield treatment. J Mol Genet Med 9: 179.

[31] Trivedi MK, Branton A, Trivedi D, Nayak G, Charan S, Jana S (2015) Phenotyping and 16S rDNA analysis after biofield treatment on Citrobacter braakii: A urinary pathogen. J Clin Med Genom 3: 129.

[32] Trivedi MK, Tallapragada RM, Branton A, Trivedi D, Nayak G, Latiyal O, Jana S (2015) Physical, atomic and thermal properties of biofield treated lithium powder. J Adv Chem Eng 5: 136.

[33] Trivedi MK, Tallapragada RM, Branton A, Trivedi D, Nayak G, Latiyal O, Mishra RK, Jana S (2015) Physicochemical characterization of biofield treated calcium carbonate powder. American Journal of Health Research 3: 368-375.

[34] Trivedi MK, Branton A, Trivedi D, Nayak G, Mondal SC, Jana S (2015) In vitro evaluation of biofield treatment on viral load against human immunodeficiency-1 and cytomegalo viruses. American Journal of Health Research. 3: 338-343.

[35] Trivedi MK, Patil S, Shettigar H, Bairwa K, Jana S (2015) Phenotypic and biotypic characterization of Klebsiella oxytoca: An impact of biofield treatment. J Microb Biochem Technol 7: 203-206.

[36] Chereson R (2009) Bioavailability, bioequivalence, and drug selection. In: Makoid CM, Vuchetich PJ, Banakar UV (Eds) Basic pharmacokinetics (1st Edn) Pharmaceutical Press, London.

[37] Trivedi MK, Mohan TRR (2016) Biofield energy signals, energy transmission and neutrinos. American Journal of Modern Physics 5: 172-176.

[38] Trivedi MK, Branton A, Trivedi D, Nayak G, Lee AC, Hancharuk A, Sand CM, Schnitzer DJ, Thanasi R, Meagher EM, Pyka FA, Gerber GR, Stromsnas JC, ShapiroJM, Streicher LN, Hachfeld LM, Hornung MC, Rowe PM, Henderson SJ, Benson SM, Holmlund ST, Salters SP, Panda P, Jana S (2017) Investigation of physicochemical, spectral, and thermal properties of sodium selenate treated with the Energy of Consciousness (The Trivedi Effect®). American Journal of Life Sciences 5: 27-37.

[39] Trivedi MK, Branton A, Trivedi D, Nayak G, Nykvist CD, Lavelle C, Przybylski DP, Vincent DH, Felger D, Konersman DJ, Feeney EA, Prague JA, Starodub JL, Rasdan K, Strassman KM, Soboleff L, Mayne MA, Keesee MM, Pillai PN, Ansley PC, Schmitz RD, Sodomora SM, Sethi KK, Panda P, Jana S (2017) Evaluation of the physicochemical, spectral, and thermal properties of sodium selenate treated with the Energy of Consciousness (The Trivedi Effect®). Advances in Bioscience and Bioengineering 5: 12-21.

[40] Trivedi MK, Sethi KK, Panda P, Jana S (2017) Physicochemical, thermal and spectroscopic characterization of sodium selenate using XRD, PSD, DSC, TGA/DTG, UV-vis, and FT-IR. Marmara Pharmaceutical Journal 21/2: 311-318.

[41] Alexander L, Klug HP (1950) Determination of crystallite size with the X-Ray Spectrometer. J App Phys 21: 137.

[42] Langford JI, Wilson AJC (1978) Scherrer after sixty years: A survey and some new results in the determination of crystallite size. J Appl Cryst 11: 102-113.

[43] Inoue M, Hirasawa I (2013) The relationship between crystal morphology and XRD peak intensity on CaSO4.2H2O. J Crystal Growth 380: 169-175.

[44] Raza K, Kumar P, Ratan S, Malik R, Arora S (2014) Polymorphism: The phenomenon affecting the performance of drugs. SOJ Pharm Pharm Sci 1: 10.

[45] Thiruvengadam E, Vellaisamy G (2014) Polymorphism in pharmaceutical ingredients a review. World Journal of Pharmacy and Pharmaceutical Sciences 3: 621-633.

[46] Brittain HG (2009) Polymorphism in pharmaceutical solids in Drugs and Pharmaceutical Sciences, volume 192, 2nd Edn, Informa Healthcare USA, Inc., New York.

[47] Blagden N, de Matas M, Gavan PT, York P (2007) Crystal engineering of active pharmaceutical ingredients to improve solubility and dissolution rates. Adv Drug Deliv Rev 59: 617-630.

[48] Khadka P, Ro J, Kim H, Kim I, Kim JT, Kim H, Cho JM, Yun G, Lee J (2014) Pharmaceutical particle technologies: An approach to improve drug solubility, dissolution and bioavailability. Asian J Pharm Sci 9: 304-316.

[49] Kale VV, Gadekar S, Ittadwar AM (2011) Particle size enlargement: Making and understanding of the behavior of powder (particle) system. Syst Rev Pharm 2: 79.

[50] Podczeck F, Mia Y (1996) The influence of particle size and shape on the angle of internal friction and the flow factor of unlubricated and lubricated powders. Int J Pharm 144: 187-194.

[51] Stuart BH (2004) Infrared spectroscopy: Fundamentals and applications in Analytical Techniques in the Sciences. John Wiley & Sons Ltd., Chichester, UK.

[52] Bajaj S, Singla D, Sakhuja N (2012) Stability testing of pharmaceutical products. J App Pharm Sci 2: 129-138.